Dispersed Phase Mass Transfer During Drop Formation and Coalescence in Liquid-Liquid Extraction

A. H. P. SKELLAND and SARDUL S. MINHAS

Department of Chemical Engineering
University of Notre Dame, Notre Dame, Indiana 46556

Rates of mass transfer during drop formation and coalescence were investigated for three dispersed phase-controlled liquid systems, one binary (ethyl acetate-water) and two ternary (acetic acid-chlorobenzene-water and acetic acid-50% by volume mixture of carbon tetrachloride and nujol-water). A calculation procedure was devised to isolate these end effects. The measured rates during drop formation were in general greater than predicted by various theoretical models, including those by Heertjes et al. and Ilkovic; and measurements during drop coalescence were in general lower than predicted by the simplified penetration theory model of Johnson and Hamielec. The results were statistically correlated with average absolute deviations of 26.2 and 25.4%, respectively, for drop formation and coalescence.

Liquid-liquid extraction is an important diffusional separation operation which employs several types of equipment, such as mixer-settlers, packed columns, agitated towers, spray columns, and perforated plate columns. In these, mass transfer is facilitated by dispersing one liquid phase in the other. The factors affecting the design of such equipment have received considerable attention recently. The totally empirical nature of design of former years, wherein the local effects within the apparatus were ignored in an attempt to correlate the terminal results, has been gradually replaced by a process of estimating mass transfer rates and countercurrent capacities for the apparatus from fundamental studies and pragmatic data taken from the literature. Skelland and Cornish (38) have presented a procedure for designing perforated plate columns which avoids any need for experimentally determined stage efficiencies. The latter are expensive, inconvenient to obtain, and of uncertain validity in scaled-up application. In addition to mass transfer during drop formation and coalescence at the interface, the design procedure requires that the shape of moving drops, the drop size and terminal velocity, interfacial areas for all stages of mass transfer, and mass transfer during the free fall (or free rise) period be predicted. With the exception of the first two, quantitative relations for their estimation have been published (*11, 16, 19, 32, 33, 37, 39, 44*).

Mass transfer during drop formation and drop coalescence at an interface, the interaction between mass transfer and hydrodynamic effects in the vicinity of an interface, the distribution of drop sizes, the repeated coalescence and redispersion of drops in a dynamic environment, and the attendant effect on mass transfer and the spread of residence times in the continuous phase and of the drop population in the flow apparatus are factors still not quantitatively described or even fully understood. The first two factors are relatively more significant in perforated plate columns due to the short distance traveled by the swarms of drops between plates. The latter factors are more significant in spray columns.

The purpose of the present investigation is to obtain correlations that will predict the rate of dispersed phase

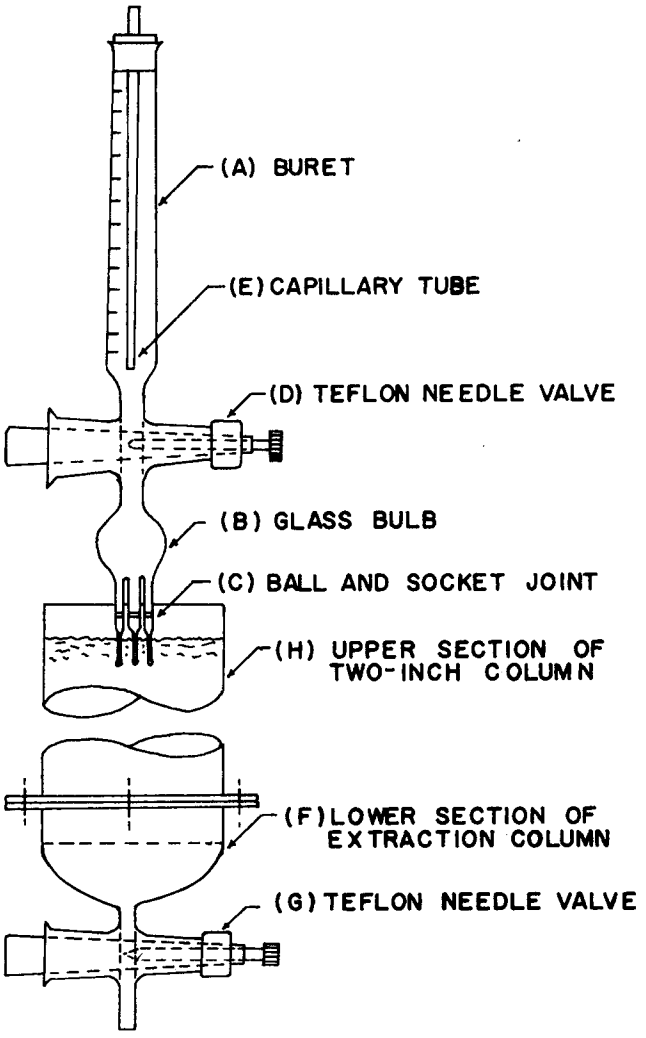

Fig. 1. Diagram of apparatus for mass transfer experiments

A. H. P. Skelland is at the University of Kentucky, Lexington, Kentucky 40506. Sardul Minhas is with Scientific Design Company, Two Park Avenue, New York, New York 10016.

TABLE 1. THEORETICAL MODELS FOR DISPERSED PHASE MASS TRANSFER DURING DROP FORMATION

Authors	Equation	Equation number	Assumed mechanism
Licht and Pansing (*27*)	$k_{df} = (6/7)(D_d/\pi\, t_f)^{1/2}$	1	The whole area ages according to penetration theory. Only area variation with time is considered.
Heertjes et al. (*17*)	$k_{df} = (24/7)(D_d/\pi\, t_f)^{1/2}$	2	Velocity of diffusion is small compared with velocity of drop growth.
Groothuis and Kramers (*13*)	$k_{df} = (4/3)(D_d/\pi\, t_f)^{1/2}$	3	Drop growth occurs by formation of fresh surface elements and there is no mixing of elements of different age.
Coulson and Skinner (*9*)	$k_{df} = 2\sqrt{3/5}\,(D_d/\pi\, t_f)^{1/2}$	4	Average time of exposure and average exposed surface are obtained by the fresh surface mechanism.
Heertjes and DeNie (*18*)	$k_{df} = 2\,(a_o/a_r + 2/3) \times (D_d/\pi\, t_f)^{1/2}$	5	Periods of rest, drop formation and the part forming the rest drop are considered separately. Based on the fresh surface mechanism.
Heertjes and DeNie (*18*)	$k_{df} = 2(7/3)^{1/2}\,(a_o/a_r + 1/3) \times (D_d/\pi\, t_f)^{1/2}$	6	Growth of surface occurs by even stretching of the diffusion layer.
Ilkovic (*20*)	$k_{df} = 1.31\,(D_d/\pi\, t_f)^{1/2}$	7	Surface stretch mechanism.

mass transfer during drop formation and drop coalescence at a liquid interface from a knowledge of the physical properties of the dispersed and continuous liquid phases and various dynamic parameters, such as the frequency of drop formation at the nozzle, drop size, and velocity.

REVIEW OF PREVIOUS WORK

Drop Formation

An extensive literature survey (*31*) showed that although several investigators have presented theoretical models governing mass transfer and made experimental observations revealing qualitative trends, no accurate means of predicting the dispersed phase mass transfer rates during drop formation have been published. These different models are summarized in Table 1. The drop is assumed to grow as a sphere and k_{df} is based on time of drop formation t_f and surface area at the point of detachment. Angelo, Lightfoot, and Howard (*2*) developed a generalized penetration theory for the surface stretch model (not included in table) which includes as a special case the more restricted situation of Ilkovic.

Heertjes et al. (*17*) demonstrated the presence of internal circulation in rapidly growing drops. Isobutanol drops colored blue with cobalt chloride were formed in a water phase. Above a certain water content in the drop the blue color changed to pink. By means of this color change they observed that drops formed in 1.3 sec. or less showed a very marked circulation, whereas no circulation occurred for formation times larger than 1.5 sec. The models in Table 1 do not consider the effect of internal circulation on mass transfer and should be expected to predict the lower limit of mass transfer during drop formation.

Much of the published experimental work has lacked a good technique for direct measurement of mass transfer during drop formation and has been confined to very large formation times (2 to 50 sec.), thus not reflecting the high transfer rates associated with circulation in growing drops being formed at higher frequency ($t_f < 1.5$ sec.). Several investigators (*26, 36, 45*) reported substantial (14 to 40%) mass transfer occurred during drop formation. The systems studied were extraction of acetic acid from methyl isobutyl ketone and benzene droplets with water (*36*) and from water drops with isopropyl ether (*26*), transfer of propionic and benzoic acids from water to benzene drops (*9*), and transfer of acetic acid out of nitrobenzene drops into water (*10*).

The measured transfer rates of Heertjes et al. (0.24 sec. $\leq t_f \leq$ 1.18 sec.) of isobutanol into water drops and vice-versa were two to five times the value predicted by their model, Equation (2). Groothuis and Kramers (*13*) observed a good agreement between their model, Equation (3), and their measurements on the amount of sulfur dioxide absorbed by individual growing drops of water. Ilkovic's expression, Equation (7), best fitted the experimental data of Popovich et al. (*35*) on the transfer of sodium iodide into isobutyl alcohol. The fresh surface model [Equation (5)] of Heertjes and DeNie provided the best fit of their data on transfer of water into growing isobutanol drops.

Drop Coalescence

Considerable literature (*1, 4* to *7, 12, 15, 21, 22, 24, 30, 43*) on the mechanism of coalescence of drops at a liquid interface exists. By contrast, information on the mass transfer aspects is scarce. Johnson and Hamielec (*23*) derived an expression for k_{dc} for the highly simplified case of a drop coalescing immediately as it reaches the boundary between the phases. The drop contents are assumed to spread out over the entire coalescence surface in a uniform layer. Mass transfer is regarded as occurring according to penetration theory and the time of exposure of the layer is taken to be the same as the time of formation of the drop.

$$k_{dc} = (D_d/\pi t_f)^{1/2} \qquad (8)$$

EXPERIMENTAL APPARATUS AND PROCEDURE

Some important considerations affecting the design of the apparatus were the effective isolation of mass transfer during

drop formation and coalescence; the surface area for coalescence per stream of drops; and hydrodynamic disturbance in the field liquid around the drop as it grows, falls, and coalesces. The technique of Licht and Conway required two extraction columns. In the first column, mass transfer occurred in all three stages of drop formation, fall, and coalescence. In the second unit, a large stopcock separated the column into upper and lower sections and the interface was maintained in the lower section. At the end of a run, the stopcock was closed and the continuous phase in the upper section was analyzed to yield mass transfer occurring during drop formation and free fall periods only. Data from identical runs made on the two columns, when extrapolated to zero height of fall, gave mass transfer which occurred during drop formation and coalescence in the first set of data, and mass transfer which occurred only during drop formation in the second set.

However, a serious drawback to this technique is apparent from the presence of a moving wake in the field fluid behind a liquid drop, as established by Magarvey and Maclatchy (29). A large part of the mass transferred from the drop to the ambient liquid is subsequently trapped in the moving wake and reaches the field liquid only when the wake is detached from the drop. This delay would attribute less than the true value of mass transferred to the drop formation and free fall periods, since part of the solute is dragged along in the wake moving with the drops through the stopcock that would otherwise isolate the coalescence effect in the bottom part of the extraction column.

An alternate method to using column 2 was therefore devised. The second set of runs was obtained in the same column used for taking runs that included all three stages of mass transfer. However, in this case the level of the interface between the coalesced layer and the continuous phase was maintained in the very narrow exit tube at the bottom end of the column. The large reduction in surface area available for mass transfer during coalescence minimized this end effect. Lindland and Terjesen (28) used a similar technique and reported errors of less than 1% if the coalescence end effect in such a set-up were neglected.

The hydrodynamic disturbance in the field liquid around the drop influences the mass transfer to or from other drops in its neighborhood, a situation characteristic of conditions in a perforated plate column. To reflect this effect and to approximate the surface area of the coalesced layer per droplet stream available in a commercial perforated plate column, the disperse liquid was distributed into three parallel streams of drops, the nozzles being set at the corners of an equilateral triangle of ¾ in. side. Using a 2-in. I.D. extraction column, the plane coalescence area per droplet stream resulting from such a pattern is about the same as in a commercial column (40, 42).

Table 2. Equilibrium Distribution of Acetic Acid Between Chlorobenzene and Water

Temperature = 23.5°C.

Conc. aqueous phase, g.-moles/ml. × 10^3	Conc. chlorobenzene phase, g.-moles/ml. × 10^3
0.6277	0.0117
2.1228	0.0858
3.4305	0.2040
4.4566	0.3248
5.4123	0.4594
6.2171	0.6099

$C_d^* = 3.264\ (C_c)^{1.70}$

Table 3. Equilibrium Distribution of Acetic Acid Between Nujol-CCl_4 and Water

Temperature = 26°C.

Conc. aqueous phase, g.-moles/ml. × 10^4	Conc. organic phase, g.-moles/ml. × 10^6
1.070	0.828
1.530	0.968
2.106	1.400
2.240	1.169
2.940	1.642
4.550	2.068

$C_d^* = 3.283 \times 10^{-4}\ (C_c)^{0.66}$

Experimental Apparatus

The apparatus is shown in Figure 1. The method of Mariotte [insertion of an open capillary tube (E) in the buret, through a stopper] was used for maintenance of constant pressure head at the lower end of the buret. Pyrex glass extraction columns of 2 in. I.D. and with effective fall heights of 6, 14, 20, 26, and 32 cm. were used. Great care was taken to avoid contamination of the apparatus by foreign substances. Teflon valves eliminated the problem of contamination with stopcock grease, and the whole apparatus was frequently rinsed with hot chromic acid solution.

Materials

One binary and two ternary liquid systems were studied. The Colburn and Welsh (8) two-component technique was used for the binary system, causing most resistance to mass transfer to lie in the disperse phase. The system chosen, ethyl acetate-water (water drops falling through ethyl acetate saturated with water), satisfied the requirements of this technique, namely, that the saturation concentration in the continuous phase must not be high, and the saturation concentration in the disperse phase must be large enough to obtain a measurable rate of mass transfer.

The two ternary systems, with the solute mentioned first, followed by the disperse and continuous phases, respectively, were acetic acid-chlorobenzene-water and acetic acid-50% by volume mixture of carbon tetrachloride and nujol-water. For the operating range of the continuous phase composition, the solubility of acetic acid favored the continuous phase on the average by a ratio of 54 to 1 for the chlorobenzene system and 125 to 1 for the nujol-carbon tetrachloride system, indicating that the continuous phase resistance to mass transfer was negligible. Nujol was used to obtain a good range of disperse phase viscosity.

The distribution of acetic acid between the two phases for each of the ternary systems is presented in Tables 2 and 3, and can be represented by an equation of the type

$$C_d^* = a'\ (C_c)^n \qquad (9)$$

Table 4. Physical Properties of the Three Experimental Systems

System	ρ_d, g./ml.	ρ_c, g./ml.	μ_d, cp.	μ_c, cp.	σ, dyne/cm.	$D_d \times 10^5$ sq. cm./sec.	T, °C.
Ethyl acetate-water	0.9979	0.9024	0.9913	0.4670	6.226	0.83289	22.0
Acetic acid-chlorobenzene-water	1.1005	0.9978	0.7550	0.8760	24.280	2.07200	23.5
Acetic acid-50% by volume mixture of CCl_4 and nujol-water	1.2214	0.9978	3.7030	0.9100	24.880	0.69511	26.0

Physical Properties

For the two ternary systems, the measurements of physical properties were made on the disperse and continuous phases as they would be at the start of each mass transfer experiment, mutually saturated, with acetic acid present only in the disperse phase. In the case of the binary system all measurements were made on pure disperse and saturated continuous phase liquids, with the exception of interfacial tension, in which case both liquids were mutually saturated. The data appear in Table 4.

Interfacial tensions were measured on a Du Nuoy Interfacial Tensiometer, K8600. An average value of 10 observations, which gave the highest value of interfacial tension, was taken. Lower values were considered unreliable because the film could be ruptured by external disturbances before maximum tension could be applied on the ring. An Ostwald-Fenske type capillary tube viscometer of ASTM No. 100 was used for measuring viscosities. Density measurements were made on a pychnometer. Molecular diffusivity for the second system (acetic acid-chlorobenzene-water) was estimated from the King and Mao (25) correlation and the Wilke and Chang (46) correlation was used for estimating diffusivity for the third system (acetic acid-carbon tetrachloride and nujol-water). Pasternak and Gauvin's (34) experimentally determined value of the liquid diffusion coefficient of ethyl acetate diffusing through water at 25°C. was usd for the binary system after making a temperature correction.

Composition Analysis

For the binary system, solute concentrations in the disperse phase were determined by refractive index with a previously determined calibration curve. A Pulfrich Refractometer was used; the readings of the refractive indices were exact within five units of the fifth decimal. The amount of acetic acid in the continuous phase while working with the ternary systems was obtaind by titration against a standard solution of sodium hydroxide.

Procedure

A vacuum bulb was used to draw the phase to be dispersed up through the nozzles and the glass bulb B into the buret. This eliminated the possibility of air bubbles becoming trapped in the delivery system and allowed droplets to form at the three nozzle tips at equal frequency. The total duration of a run was timed with a stopwatch. A second stopwatch was used to time the formation of, say, 10 drops for each nozzle about three or four times during a run. From the times of drop formation for each nozzle, the total volume of disperse phase used, and the measured duration of the run, the average equivalent drop diameter (the diameter of a sphere which has the same volume as that of the drop) and a weighted average drop formation time could be calculated.

The level of the disperse phase that collected in the cone at the lower end of the extraction column was allowed to build up. When it reached the top of the cone the disperse phase was drained off through the control valve G at a rate that kept the interface constantly at the above level until the end of the run. In the case of the binary system the drained disperse phase was sampled several times and analyzed for its ethyl acetate content through refractive index measurement. After about 30 ml. had passed, the composition became steady and the final value was used for computing the solute transferred into the water drops, the corresponding height of fall being the distance between the nozzle tips and the final level of the interface. For experiments with the ternary systems at the end of each run the remaining disperse phase was analyzed volumetrically for the total solute transferred during the run. Integrated dispersed volume average height of fall and surface area of coalescence were used for calculations.

Droplet fall velocities were obtained with a stopwatch for a free fall distance of 54 cm. Experimental runs were made for five different heights of fall, three drop sizes, and three drop formation times (approximately 0.5, 1.0, and 1.5 sec.). The mean temperatures at which mass transfer experiments were carried out were 22°, 23.5°, and 26°C. for systems 1, 2, and 3, respectively.

For the second set of runs where mass transfer during coalescence was sought to be minimized, the procedure was identical except that the interface of the coalesced layer with the continuous phase was maintained in the narrow exit tube at the bottom of the extraction column.

Calculation of Disperse Phase Coefficients of Mass Transfer, k_{df}, and k_{dc}

In the past, experimental data have been processed in two ways, the theoretical basis of which can be traced to several mathematical models describing mass transfer in drops during the free fall period. However, the Licht and Conway technique of plotting the log fraction solute unextracted versus drop-fall time or column height and graphical extrapolation procedure to zero height has been shown to be invalid by Licht and Pansing (27). The other method, developed by Johnson and Hamielec (23), proposes that when data are plotted in their special manner, straight lines should result, enabling extrapolation to zero height of fall for isolating mass transfer in each of the three stages. The plots involved are E_T versus $\sqrt{t}$ for $E_m < 0.5$ and $\ln(1 - E_T)$ versus t for $E_m > 0.5$, where E_T and E_m are total fractional extraction and that during the free-fall period respectively. Two different approximations of a theoretical expression for free-fall mass transfer for the above two cases were used in their procedure; however, several systems were found not to plot linearly (39) and the method is not of general application.

We devised a new method of calculation. In the following, k_{df}, k_{dr}, and k_{dc} are defined for arithmetic averages of the concentration driving forces at the start and end of the respective periods. The surface area used is that of a sphere having the same volume as that of the fully grown drop for k_{df}, that of an oblate spheroid having the same volume as that of the falling drop for k_{dr}, and that of a plane area of interface per droplet stream for k_{dc}. Finally, k_{df} and k_{dc} are both based on the time of drop formation.

The amount extracted from a single drop in all three stages is given by

$$S_d = k_{df}\, a_f\, t_f\, (\Delta C)_f + k_{dr}\, a_r\, t_r\, (\Delta C)_r + k_{dc}\, a_c\, t_f\, (\Delta C)_c \tag{10}$$

By definition

$$(\Delta C)_f = \frac{1}{2}(C_{d0} + C_{d1}) - C_d^* \tag{11}$$

The rate expression and the material balance are now combined.

$$k_{df}\, a_f\, t_f\, (\Delta C)_f = v_d\, (C_{d0} - C_{d1}) \tag{12}$$

From Equations (11) and (12)

$$(\Delta C)_f = \Delta C \frac{2}{2 + (k_{df}/v_d) a_f t_f} \tag{13}$$

where

$$\Delta C = C_{d0} - C_d^* \tag{14}$$

Continuation of this treatment into the free-fall and coalescence periods leads to the following expressions for $(\Delta C)_r$ and $(\Delta C)_c$:

$$(\Delta C)_r = \Delta C \cdot 2 \frac{1 - \dfrac{2\,(k_{df}/v_d) a_f t_f}{2 + (k_{df}/v_d) a_f t_f}}{2 + (k_{dr}/v_d) a_r t_r} \tag{15}$$

$$(\Delta C)_c = \Delta C \cdot 2 \left[\frac{4 \dfrac{1 - \dfrac{2\,(k_{df}/v_d) a_f t_f}{2 + (k_{df}/v_d) a_f t_f}}{2 + (k_{dr}/v_d) a_r t_r} - \frac{2 - (k_{df}/v_d) a_f t_f}{2 + (k_{df}/v_d) a_f t_f}}{2 + (k_{dc}/v_d) a_c t_f} \right] \tag{16}$$

For purposes of simplification, define the following dimensionless parameters:

$$T = (k_{df}/v_d) a_f t_f \tag{17}$$

$$U = (k_{dc}/v_d) a_c t_f \tag{18}$$

Equation (10) then takes the form

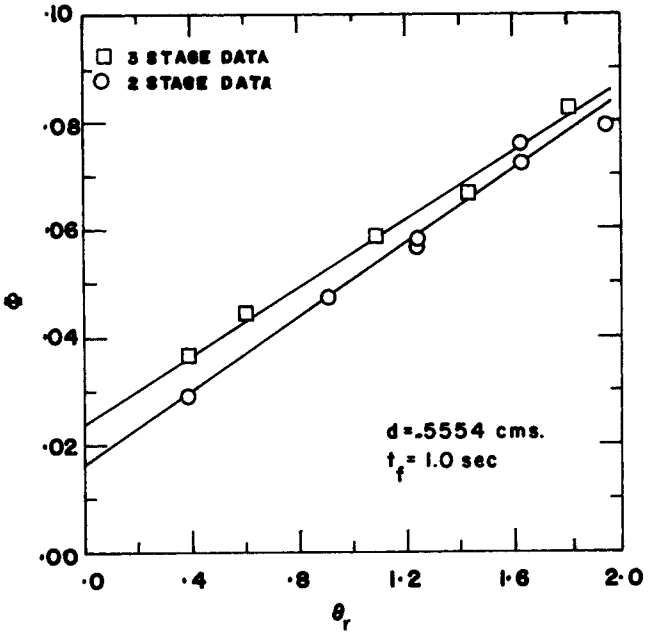

Fig. 2. Plot of the data of Nujol system

$$\frac{(2 + (k_{dr}/v_d)a_r t_r)\, S_d}{\Delta C} = 4 v_d \left(\frac{T}{2+T} + \frac{2-T}{2+T} \cdot \frac{U}{2+U} \right) + 2a_r \left(\frac{2}{2+T} - \frac{2-T}{2+T} \cdot \frac{U}{2+U} \right) k_{dr} t_r \quad (19)$$

An empirical expression for k_{dr} that would provide a satisfactory fit with the free-fall experimental data is now introduced. Based on the dimensionless group correlation of Skelland and Wellek (39), the dependence of k_{dr} on the free-fall contact time is described by

$$k_{dr} = \alpha\, t_r^{\beta} \quad (20)$$

$$\theta_r = t_r^{1+\beta} \quad (21)$$

Equation (19) can now be rewritten as

$$\Phi = 4 v_d \left(\frac{T}{2+T} + \frac{2-T}{2+T} \cdot \frac{U}{2+U} \right) + 2\alpha a_r \left(\frac{2}{2+T} - \frac{2-T}{2+T} \cdot \frac{U}{2+U} \right) \cdot \theta_r \quad (22)$$

where

$$\Phi = \frac{(2 + \alpha a_r\, \theta_r / v_d)\, S\, v_d}{\Delta C\, V_R} \quad (23)$$

Equation (22) indicates that for a set of experimental runs where only the height of free fall is varied, the plot of Φ versus θ_r should be linear. For the set of runs in which mass transfer during coalescence was minimized, Equation (22) simplifies to

$$\Phi = \frac{4 v_d T}{2+T} + \frac{4 \alpha a_r}{2+T} \cdot \theta_r \quad (24)$$

Let I_f and $I_{f,c}$ denote the intercept on the Φ axis for set II runs (coalescence minimized) and set I runs (all three stages included). Expressions for k_{df} and k_{dc} are readily obtained

$$k_{df} = \frac{v_d}{a_f t_f} \cdot \frac{2 I_f}{4 v_d - I_f} \quad (25)$$

$$k_{dc} = \frac{2 v_d}{a_c t_f} \cdot \frac{2 I_{f,c} + (k_{df}/v_d) a_f t_f (I_{f,c} - 4 v_d)}{8 v_d - 2 I_{f,c} - (k_{df}/v_d) a_f t_f I_{f,c}} \quad (26)$$

Before the data can be plotted in accordance with the above equations, the constants α and β in Equation (20) for each set of runs must be determined. This was done from runs in which the coalescence end effect was minimized. The average droplet concentration during the free fall of any longer column was considered to vary from the exit concentration of the shortest column, C_{di} to the exit concentration from any longer column C_{df}. The solute transferred S_{drc} was taken to be the difference between that for a longer column and that for the shortest column; the corresponding time of contact t_{rc} was similarly defined.

$$k_{dr} = \frac{S_{drc}}{t_{rc}\, a_r \left(\frac{1}{2} (C_{di} + C_{df}) - C_d^* \right)} \quad (27)$$

A least-squares analysis of k_{dr} and t_{rc} values for each set of runs yielded values of α and β providing the best fit.

The droplet eccentricities were calculated from the Wellek, Agrawal, and Skelland correlation (*44*); a_r was readily calculated from the surface of a spherical drop of equal volume using the relationship presented by Garner and Tayeban (*11*).

EXPERIMENTAL RESULTS

Before discussing the detailed results for drop formation and coalescence mass transfer, it is pertinent to report on the effectiveness of the above proposed method of plotting data. Two representative sets of runs are plotted in Figure 2. These were taken on the Nujol system and correspond to an average drop diameter of 0.5554 cm. and t_f of 1.0 sec.

Table 5 lists the range of experimental variables, for example, nozzle diameter, drop diameter at detachment, drop formation time, and terminal velocity for each system. For the entire range of nozzle velocities, all drops formed at the nozzle tip.

Experimental raw data are available elsewhere (*31*).

Mass Transfer During Drop Formation

For the binary system the drop diameter at detachment ranged between 0.3673 and 0.5323 cm. Bigger drops were formed in the ternary systems due to higher values of interfacial tension. The variation of drop size in the chlorobenzene system was from 0.5633 to 0.7764 cm. and for the Nujol system drop sizes ranged between 0.4875 and 0.6491 cm. Fractional extraction during drop formation varied as follows: ethyl acetate system, 3.07 to 17.15%; chlorobenzene system, 23.23 to 39.25%; Nujol system, 9.11 to 13.75%.

The different theoretical models discussed earlier are reduced to a common form:

Table 5. Range of Measured Variables

Variable	System: Ethyl acetate-water	System: Acetic acid-chlorobenzene-water	System: Acetic acid-nujol-CCl_4-water
d, cm.	0.367-0.532	0.563-0.776	0.488-0.649
d_n, mm.	1.24-2.52	0.74-2.52	0.74-2.52
t_f, sec.	0.505-1.507	0.505-1.513	0.498-1.502
v_t, cm./sec.	8.415-9.266	11.027-12.040	14.652-15.208
k_{df}, cm./sec. $\times 10^2$	0.536-1.341	2.784-8.449	0.892-2.066
k_{dr}, cm./sec. $\times 10^2$	0.895-1.502	0.791-4.277	1.299-2.365
k_{dc}, cm./sec. $\times 10^3$	0.274-4.208	1.820-10.398	0.283-0.853

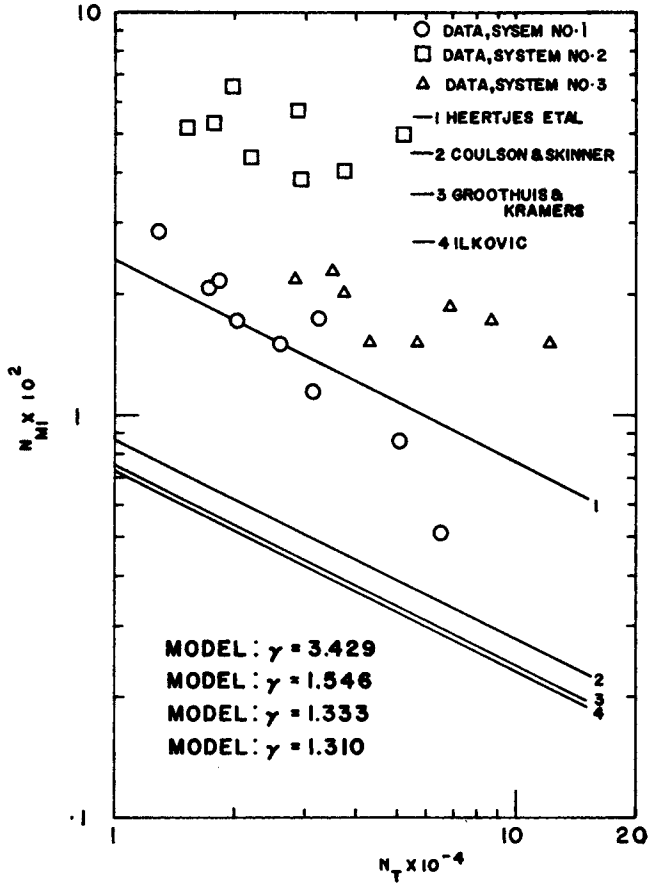

Fig. 3. Comparison of observed and theoretical rates of mass transfer in drop formation.

$$k_{df} = \gamma \left(\frac{D_d}{\pi t_f}\right)^{1/2} \tag{28}$$

The dimensionless group N_{MI} is defined as follows

$$N_{MI} = k_{df}\, t_f/d \tag{29}$$

Thus

$$N_{MI} = \frac{\gamma}{\sqrt{\pi}} N_T^{-0.5} \tag{30}$$

where

$$N_T = \frac{d^2}{t_f D_d} \tag{31}$$

The four theoretical models of Coulson and Skinner, Heertjes et al., Groothuis and Kramers, and Ilkovic and all the experimental mass transfer data during drop formation for the three systems are plotted in Figure 3. The k_{df} values in the latter are adjusted and defined for ΔC rather than $(\Delta C)_f$ to put them on a common basis with k_{df} of Equation (28). This figure shows that the observed mass transfer is considerably higher than the theoretically predicted values and the experimental points for the three systems form three separate clusters. The former observation is explained by the noninclusion in the models of internal circulation caused by the impinging jet while the drop grows, interfacial turbulence, influence of the rest drop remaining after detachment, and disturbance associated with drop detachment. The latter observation indicates that a realistic model should include other parameters, such as density, viscosity, and interfacial tension.

An empirical correlation of the results was therefore attempted. The following list of variables ought to fully describe the different phenomena which influence the mass transfer during drop formation. (Solute concentration was not included because all experiments were conducted for dilute concentrations and maximum concentration of acetic acid in the dispersed phase was 1.6 and 2.4% by weight, respectively, for the chlorobenzene and the nujol-CCl_4 systems.)

$$k_{df} = f_n\,(t_f, d, d_n, v_n, D_d, \sigma, \rho_c, \rho_d, \Delta\rho, \mu_c, \mu_d) \tag{32}$$

The data were correlated by 32 dimensionless variations of Equation (32), using multiple regression analysis on the University of Notre Dame Univac 1107 digital computer. The following was the best correlation and is recommended.

$$\frac{k_{df}\, t_f}{d} \quad (N_{MI})$$

$$= 0.0432 \underbrace{\left(\frac{v_n^2}{dg}\right)^{0.089}}_{(N_{Fr})} \underbrace{\left(\frac{d^2}{t_f D_d}\right)^{-0.334}}_{(N_T)} \underbrace{\left(\frac{\mu_d}{\sqrt{\rho_d\, d\sigma}}\right)^{-0.601}}_{(N_{Oh})} \tag{33}$$

The average absolute deviation from the data was 26.23%, the variance in the logarithmic form was 0.03379, and the multiple correlation coefficient was 0.8149. The 95% confidence limits on the exponents were 0.089 ± 0.017; -0.334 ± 0.048; -0.601 ± 0.060.

Equation (33) covers the following range of variables

$$0.521 \times 10^{-2} \leq N_{MI} \leq 8.140 \times 10^{-2}$$

$$0.163 \times 10^{-2} \leq N_{Fr} \leq 0.3955$$

$$1.286 \times 10^{4} \leq N_T \leq 12.131 \times 10^{4}$$

$$0.165 \times 10^{-2} \leq N_{Oh} \leq 0.961 \times 10^{-2}$$

Expansion of Equation (33) in terms of the primary variables results in an exponent of 0.334 for solute diffusivity in the dispersed phase. Although this is smaller than the value predicted by penetration theory (0.5) or

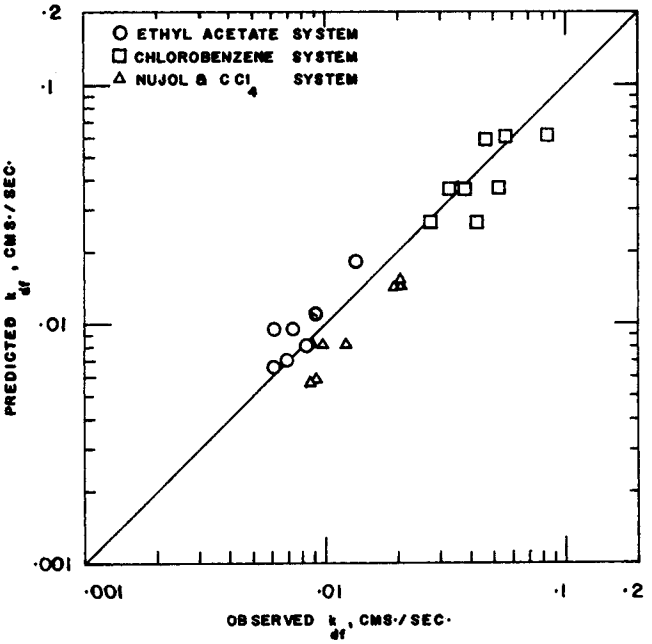

Fig. 4. Correlation: mass transfer during drop formation.

two-film theory (1.0), previous investigators (*14*) have reported values of 0.0, 0.16, 0.37, 0.5, and 0.66 from their experiments.

Equation (33) is represented graphically in Figure 4. It may be noted that this correlation represents the overall mass transfer occurring during drop formation, which includes mass transfer during drop growth, during the detachment of the drop, and the influence of the rest drop left behind after detachment.

Mass Transfer During Drop Coalescence at a Liquid Interface

Visual observations indicated that chlorobenzene drops were the quickest to coalesce on reaching the liquid interface—the process was almost instantaneous. The nujol-CCl_4 system drops took the longest and water drops had intermediate rest times. Especially in the nujol-CCl_4 system, drops tended to pile up and form more than one layer at the phase boundary.

Mass transfer during drop coalescence differed considerably from that during drop formation. The ratio of solute transferred during drop formation to that transferred during drop coalescence (taken for runs of 32 cm. fall height) varied as follows: ethyl acetate system, 1.21 to 5.56; chlorobenzene system, 3.41 to 9.88 and nujol-CCl_4 system, 3.64 to 11.52. This contradicts the contentions of Licht and Conway (*26*) and Coulson and Skinner (*9*), who appeared to observe nearly equal amounts of mass transfer in these two stages. The findings of Licht and Conway (*26*) must be held invalid because they purported to separate end effects in columns fitted with a large stopcock, ignoring the presence of a moving wake which follows each drop. This wake carried some of the solute transferred from the drops above the stopcock to column regions below the stopcock, as discussed earlier in this paper. The inadmissibility of end effects found using the Licht and Conway technique was also pointed out by Licht and Pansing (*27*). Indeed, the relatively small end effect for coalescence compared to formation is corroborated by the findings of Angelo and Lightfoot (*3*), who successfully correlated their results for formation + rise + coalescence by neglecting transfer during coalescence in their high interfacial tension systems. Coulson and Skinner (*9*) formed drops at a constant rate and then withdrew them into the nozzle at the same rate before they could break away. They assumed that transfer rates during formation and withdrawal were equal, so that transfer during formation was taken to be half that measured during formation and withdrawal. Baird (*3a*), however, showed from theoretical considerations that their assumption of equal transfer rates during formation and withdrawal is invalid; he found that 70.6% of the extraction occurs during formation, rather than the 50% assumed by Coulson and Skinner.

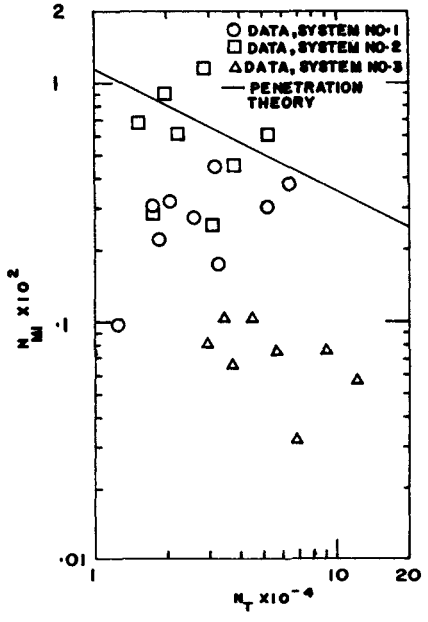

Fig. 5. Comparison of observed and theoretical rates of mass transfer in drop coalescence.

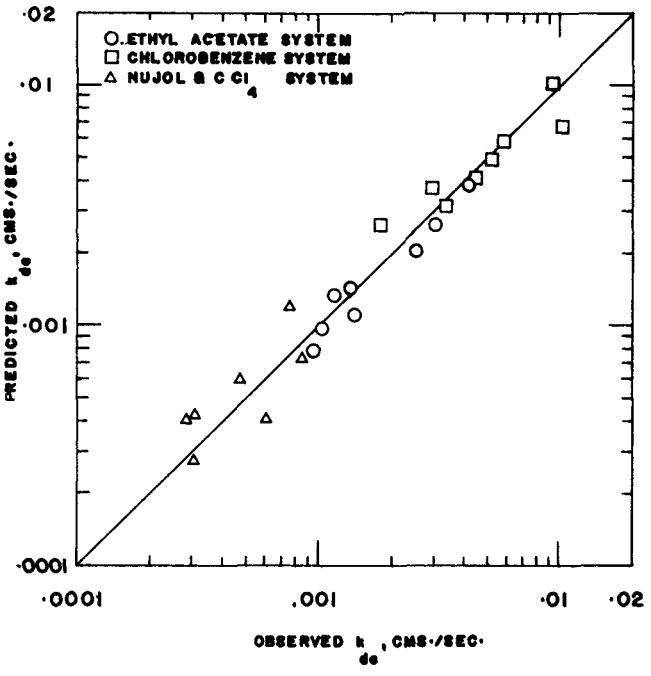

Fig. 6. Correlation: mass transfer during drop coalescence.

It is evident, therefore, that the seeming conflict with some previous findings is more apparent than real.

A modified form of the findings of Licht and Conway and Coulson and Skinner regarding equal amounts of mass transfer in the two stages was given by Treybal (*41*) as

$$k_{df}\, a_f = k_{dc}\, a_c \tag{34}$$

This was found to be invalid for the present results, as well as those of Angelo and Lightfoot (*3*), as discussed above.

The expression for k_{dc} according to penetration theory [Equation (8)] is rewritten in terms of dimensionless groups N_{MI} and N_T:

$$N_{MI} = \frac{2}{\sqrt{\pi}}\, N_T^{-0.5} \tag{35}$$

where

$$N_{MI} = k_{dc}\, t_f/d \tag{36}$$

The penetration theory result and the experimental data are plotted in Figure 5 (the measured k_{dc} values were adjusted for the initial concentration driving force). The solid line with a slope of $-\frac{1}{2}$ represents the penetration theory. It appears to provide a good fit of the data for the chlorobenzene system (two points excepted). The unsteady diffusion mechanism assumed by Johnson and Hamielec therefore seems to be a reasonable approximation when the coalescence of drops is instantaneous. The observed mass transfer rates for the other two systems, in

which drops exhibited significant rest times at the interface, are considerably smaller than predicted by penetration theory.

To correlate the measured rate data, k_{dc} was expressed as a function of the following primary variables

$$k_{dc} = f\,(t_f, d, v_t, D_d, \sigma, \rho_c, \rho_d, \Delta\rho, \mu_c, \mu_d) \qquad (37)$$

The data were correlated by 25 dimensionless variations of Equation (37). The correlating procedure was the same as that for mass transfer during drop formation and the following correlation is recommended.

$$\frac{k_{dc}\,t_f}{d}\ (N_{MI}) = 0.1727 \underbrace{\left(\frac{\mu_d}{\rho_d D_d}\right)^{-1.115}}_{(N_{Sc})} \underbrace{\left(\frac{\Delta\rho\, g\, d^2}{\sigma}\right)^{1.302}}_{(N_{Bo})} \underbrace{\left(\frac{v_t^2\, t_f}{D_d}\right)^{0.146}}_{(N_1)} \qquad (38)$$

The average absolute deviation from the data was 25.44%, variance in the logarithmic form was 0.0229, and the multiple correlation coefficient was 0.9441. The 95% confidence limits on the exponents were -1.115 ± 0.212; 1.302 ± 0.144; 0.146 ± 0.044.

The correlation covered the following range of variables

$$\begin{aligned} 0.032 \times 10^{-2} &\leq N_{MI} < 1.334 \times 10^{-2} \\ 331 &\leq N_{Sc} \leq 4362 \\ 1.314 &\leq N_{Bo} \leq 4.169 \\ 0.208 \times 10^{7} &\leq N_1 < 5.007 \times 10^{7} \end{aligned}$$

Equation (38) is represented graphically in Figure 6 where the predicted values of k_{dc} have been plotted against the measured values.

ACKNOWLEDGMENT

The financial support of the National Science Foundation (grant GK-2846) is gratefully acknowledged. Louis Joseph of the University of Notre Dame Computing Centre gave assistance in the use of the BMD03R program.

NOTATION

a' = constant in Equation (9)
a = surface area per drop, sq.cm.
a_0 = surface area of a rest drop, sq.cm
a_r = surface area of the drop at detachment, sq.cm.
C = concentration of solute in one of the two phases, g.-moles/ml.
C_{d0} = solute concentration in dispersed phase before drop formation begins, g.-moles/ml.
C_{d1} = average solute concentration in drop at detachment, g.-moles/ml.
D = volumetric diffusivity, sq.cm./sec.
d = equivalent drop diameter, cm.
d_n = inside diameter of nozzle tip, cm.
E = fractional extraction of solute, $(C_{d0} - C_{d1})/(C_{d0} - C_d^*)$
g = acceleration due to gravity, cm./sec.^{2}
I_f = intercept on the Φ axis for the two-stage runs
$I_{f,c}$ = intercept on the Φ axis for the three-stage runs
k = average individual mass transfer coefficient, cm./sec.
N_1 = $(v_t^2\, t_f/D_d)$
N_{Bo} = Bond number, $(\Delta\rho\, g d^2/\sigma)$
N_{Fr} = Froude number, (v_n^2/dg)
N_{MI} = mass transfer group, $(k_{df}\, t_f/d)$ and $(k_{dc}\, t_f/d)$
N_{Oh} = Ohnesorge number, $(\mu_d/\sqrt{\rho_d d\sigma})$
N_{Sc} = Schmidt number, $(\mu_d/\rho_d D_d)$
N_T = dimensionless time group, $(d^2/t_f\, D_d)$
n = exponent in Equation (9)
S = solute transferred in a run, g.-moles
S_d = solute transferred per drop, g.-moles
T = dimensionless parameter defined by Equation (17)
t = time, sec.
U = dimensionless parameter defined by Equation (18)
V_R = volume dispersed in a run, cc.
v_d = volume of a drop, cc.
v_n = velocity of liquid through nozzle, cm./sec.
v_t = rate of fall of drops through continuous phase, cm./sec.

Greek Letters

α, β = constants in Equation (20)
γ = common coefficient in Equation (28) for comparing models of mass transfer during drop formation
ΔC = concentration driving force for mass transfer, g.-moles/ml.
$\Delta\rho$ = difference in the densities of two phases, g./cc.
σ = interfacial tension, dynes/cm.
Φ = parameter representing solute transferred in an experimental run, defined by Equation (23)
θ_r = parameter representing time of fall of a drop, defined by Equation (21)
μ = viscosity, poises
ρ = density, g./cc.

Subscripts

c = continuous phase
c = coalescence
d = dispersed phase
f = formation
i = evaluated at initial state
r = free fall

Superscript

* refers to composition in equilibrium with the other phase

LITERATURE CITED

1. Allan, R. S., and S. G. Mason, *Trans. Faraday Soc.*, **57**, 2027 (1961).
2. Angelo, J. B., E. N. Lightfoot, and D. W. Howard, *AIChE J.*, **12**, 751 (1966).
3. Angelo, J. B., and E. N. Lightfoot, *ibid.*, **14**, 531 (1968).
3a. Baird, M. I. H., *Chem. Eng. Sci.*, **9**, 267 (1959).
4. Brown, A. H., and C. Hanson, *Brit. Chem. Eng.*, **11**, 695 (1966).
5. ———, *Trans. Faraday Soc.*, **61**, 1754 (1965).
6. Charles, G. E., and S. G. Mason, *J. Colloid. Sci.*, **15**, 105 (1960).
7. *Ibid.*, 236 (1960).
8. Colburn, A. P., and D. B. Welsh, *Trans. Am. Inst. Chem. Eng.*, **38**, 179 (1942).
9. Coulson, J. M., and S. J. Skinner, *Chem. Eng. Sci.*, **1**, 197 (1952).
10. Garner, F. H., and A. H. P. Skelland, *Ind. Eng. Chem.*, **46**, 1255 (1954).
11. Garner, F. H., and M. Tayeban, *Anal. Real Soc. Espan. Fis. Quim., Ser. B*, **LVI** (8), 479 (1960).

12. Gillespie, T., and E. Rideal, *Trans. Faraday Soc.*, **52**, 173 (1956).
13. Groothuis, H., and H. Kramers, *Chem. Eng. Sci.*, **4**, 17 (1955).
14. Hanson, C., *Chem. Eng.*, 135 (Sept. 1968).
15. Hartland, S., *Chem. Eng. Sci.*, **22**, 1675 (1967).
16. Hayworth, C. B., and R. E. Treybal, *Ind. Eng. Chem.*, **42**, 1174 (1950).
17. Heertjes, P. M., W. A. Holve, and H. Talsma, *Chem. Eng. Sci.*, **3**, 122 (1954).
18. Heertjes, P. M., and L. H. De Nie, *ibid.*, **21**, 755 (1966).
19. Hu, S., and R. C. Kintner, *AIChE J.*, **1**, 42 (1955).
20. Ilkovic, D., *Collection Czech. Chem. Commun.*, **6**, 498 (1934).
21. Jeffreys, G. V., and J. L. Hawksley, *AIChE J.*, *11*, 413 (1965).
22. Jeffreys, G. V., and G. B. Lawson, *Trans. Inst., Chem. Eng.*, **43**, T. 294 (1965).
23. Johnson, A. I., and A. E. Hamielec, *AIChE J.*, *6*, 145 (1960).
24. Katalinic, M. A., *Physik*, **38**, 511 (1926).
25. King, C. J., L. Hsueh, and K. W. Mao, *J. Chem. Eng. Data*, **10**, 348 (1965).
26. Licht, W., and J. B. Conway, *Ind. Eng. Chem.*, **42**, 1151 (1950).
27. Licht, W., and W. F. Pansing, *ibid.*, **45**, 1885 (1953).
28. Lindland, K. P., and S. G. Terjesen, *Chem. Eng. Sci.*, **5**, 1(1956).
29. Magarvey, R. H., and C. C. MacLatchy, *AIChE J.*, **14**, 260 (1968).
30. Mahajan, L. D., *Phil. Mag.*, **10**, 383 (1930).
31. Minhas, S. S., Ph.D. thesis, Univ. Notre Dame (1969).
32. Narasinga Rao, E. V. L., R. Kumar, and N. R. Kuloor, *Chem. Eng. Sci.*, **21**, 867 (1966).
33. Null, H. R., and H. F. Johnson, *AIChE J.*, **4**, 273 (1958).
34. Pasternak, I. S., and W. H. Gauvin, *Can. J. Chem. Eng.*, **38**, 35 (1960).
35. Popovich, A. T., R. E. Jervis, and O. Trass, *Chem. Eng. Sci.*, **19**, 357 (1964).
36. Sherwood, T. K., J. E. Evans, and J. V. A. Longcor, *Ind. Eng. Chem.*, **31**, 1146 (1939).
37. Skelland, A. H. P., and A. R. H. Cornish, *AIChE J.*, **9**, 73 (1963).
38. ———, *Can. J. Chem. Eng.*, **43**, 302 (1965).
39. Skelland, A. H. P. and R. M. Wellek, *AIChE J.*, **10**, 491 (1964).
40. Treybal, R. E., "Mass Transfer Operations," 1st edit., pp. 378-9, McGraw-Hill, New York (1955).
41. ———, "Liquid Extraction," 2nd edit., p. 471, McGraw-Hill, New York (1963).
42. ———, and F. E. Dumoulin, *Ind. Eng. Chem.*, **34**, 710 (1942).
43. Wark, I. W., and A. B. Cox, *Nature*, **136**, 182 (1935).
44. Wellek, R. M., A. K. Agrawal, and A. H. P. Skelland, *AIChE J.*, *12*, 854 (1966).
45. West, F. B., P. A. Robinson, A. L. Morgenthaler, T. R. Beck, and D. K. McGregor, *Ind. Eng. Chem.*, **43**, 234 (1951).
46. Wilke, C. R., and P. Chang, *AIChE J.*, *1*, 264 (1955).

Manuscript received November 3, 1970; revision received April 16, 1971; paper accepted April 20, 1971.

Solutions for Distillation Processes Treating Petroleum Fractions

D. L. TAYLOR

University of Puerto Rico, Mayaguez, Puerto Rico 00708

and W. C. EDMISTER

Oklahoma State University, Stillwater, Oklahoma 74074

The general solution for multicomponent distillation processes is used to obtain solutions for systems treating petroleum fractions. The integral technique is the basis for this adaptation. Example solutions are presented for a conventional distillation column, a distillation column with a side stream, and an absorber. The design capabilities of the general solution are illustrated by an absorber problem in which the composition of the lean vapor is specified. The amount of absorber oil, a petroleum fraction, required to accomplish this degree of separation is found.

Petroleum fractions may be regarded as continua (mixtures of an indefinite number of hydrocarbon components). On the true boiling point (TBP) distillation curve for the mixture, each component is represented by a point, as contrasted with the plateaus that appear for each component on the TBP curve for a mixture containing a finite number of components.

In distillation calculations for finite mixtures, the solutions are obtained by the use of equations involving summations. The heat balance equations and the bubble point equations are summations. For mixtures of an indefinite number of components, these equations naturally become integral in form. Edmister (*1*) has proposed the integral technique for handling such problems.

Taylor and Edmister (2) have proposed a method by which it is possible to obtain rigorous solutions for any type of distillation process by means of a single set of equations employed in a single computer program. Dis-